Landmark-Based Visual Positioning System for Automatic Guided Vehicle

Bijun Li[1], Mingyao Qi[1], Kai Zhang[1,2], Bokui Chen*

1. Division of Logistics and Transportation, Graduate School at Shenzhen, Tsinghua University, Shenzhen, China.
2. Center of Environmental Science and New Energy Technology, Tsinghua-Berkeley Shenzhen Institute, Shenzhen, China
*(Corresponding Author): Department of Computer Science, School of Computing, National University of Singapore, Singapore 117417, Singapore E-mail:chenbk@nus.edu.sg; chenssx@qq.com

ABSTRACT

The rapid development of Automatic Guided Vehicle (AGV) will soon allow many new developments in transportation systems, especially those used in warehousing and logistics. This paper proposes a vision-based positioning system for a AGV used for transporting goods in large warehouses. The AGV runs along a set route which is made up of artificial landmarks, with a camera capturing images of the ground. Every time the AGV passes through a landmark, the position and orientation deviations between the AGV and the landmark can be calculated from the local features, edges and corners. To maintain accuracy, we improve the edge extraction method based on Prewitt operator. We do not judge the edges by just roughly setting a gradient threshold, but focus on the gradient direction of each pixel. The accuracy of position deviation is 3 mm and that of orientation deviation is 1◦.

KEYWORDS: Image processing; Edge detection; Prewitt operator

INTRODUCTION

With the advent of the Internet of Things, the intelligent robots, Automatic Guided Vehicle (AGV), have been rapidly developed because of their multiple advantages. These AGVs are relatively small and can bear relatively heavy loads, meaning that they can handle shelves flexibly and transport them to different areas of a warehouse, thereby enabling the reduction of labor requirements, enhancing efficiency, and improving the storage environment. All of these help realize the “goods to people” principle in logistics and warehouse management.

In logistics and warehouse management systems, the use of AGVs has simplified the process flow and made it more efficient. However, there remain many practical problems with AGV systems, including developing scheduling rules (Gelareh et al., 2013; Hartmann, 2013), strategies for storage locations (Luo and Wu, 2015), job assignments (Angeloudis and Bell, 2010),

collaborative driving (Halle and Chaib-draa, 2005), path optimization (Fazlollahtabar and Saidi-Mehrabad, 2015), accurate positioning and motion control. As a type of mobile robot, the first problem they must solve is “where am I?” (Borenstein et al., 1996), that is to say how to position accurately. At present, many positioning methods are in use, such as Radio Frequency Identification (RFID) positioning (Bosien et al., 2008), Visible Light Communication (VLC) positioning (Jiangbo et al., 2016), ultrasonic positioning(En-xiu et al., 2005;Tabata et al.,2012), laser positioning (Bui et al., 2013; Juang and Wang, 2015; Tang et al., 2014)， and visual positioning (Hong, 2010; Carelli et al., 2002; Fontanelli et al.,2015; Ye et al.,2012). Considering our AGV’s application in large warehouses and its advantages of low cost and high performance, we select the landmark-based visual positioning method. Landmarks are placed on the ground discretely. When the AGV moves through a landmark, accurate pose information can be gained by applying the designed image-processing algorithm to the images captured by camera, since precise position and orientation data are crucial for AGV navigation. The landmark-based visual positioning method renders setting and changing an AGV path simpler and more flexible. The maintenance cost is reduced because damaged landmarks can easily be replaced and the cost of a landmark is very cheap. This method is also unaffected by electromagnets, rendering them more stable and reliable.

LANDMARK

The landmarks include encoding and function regions. The encoding region contains a QR code indicating absolute coordinates in the warehouse. The function region includes a black border and the logo “ROBU”. Shown as Figure 1, this landmark faces forward.

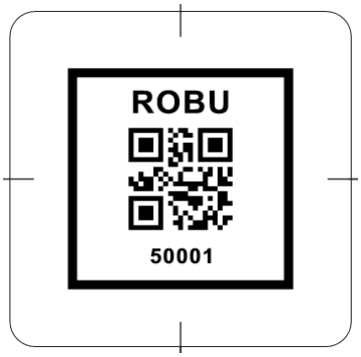

Figure 1 Landmark

IMAGE PROCESS

The landmark is pasted on the ground. The camera is mounted on the geometric center of the bottom of AGV and is consistent with the head of the AGV. The field of camera vision must be larger than the landmark.

1. A binarized image is obtained through preprocessing with adaptive threshold segmentation.

2. The second step is to identify whether the landmark is in the field of camera’s vision. We use normalized correlation coefficient matching to match the corners of the black border, seen as templates, with captured images. Four corner templates are shown in Figure 2. As long as one

of the four templates has a matching score greater than a certain threshold, it means the landmark is in the field of camera's vision. The matching results are shown in Figure 3.

Figure 2 Four corner templates

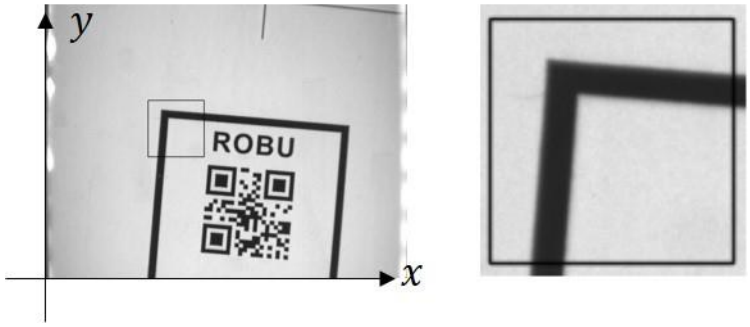

Figure 3 Matching results and matched local image

3. The third step is to decode the QR code to obtain the real position of the landmark in the warehouse.

4. The fourth step is to determine the direction of the AGV through the matching template method. The process is identical to that used in second step. The logo "ROBU" is seen as a template to match with images. If the matching score exceeds a certain threshold, the AGV and the landmark are confirmed to have same direction. The direction of the AGV's front will affect the movement of the robot.

5. Finally, the fifth step is to determine the AGV's position and orientation error relative to the landmark through complex image processing, shown in Figure 4. The orientation error, $e_{\emptyset}$, refers to the angle between the direction of the AGV's head and the forward direction of the landmark. The range of the angle deviation is $(-45°, 45°)$, increasing in the clockwise direction. Analyzing the matched local image shown in the right of Figure 3. The edge points of a straight line are extracted, and the linear function is established using the linear fitting method with those edge points. The orientation error can be calculated from the slope of the straight line, and the position error, e_x and e_y, can be calculated with the coordinates of the corner of the black border. Because of the complexity of the fifth step and must be discussed in detail.

The grey values and coordinates of pixels in the local binary image are known. The gradient value of each pixel is calculated using the first-order differential operator method. This involves determining a suitable threshold for detecting the edge points of the black border. According to the characteristics of our image, we choose Prewitt operator (Eq.1),

$$x = \begin{bmatrix} -1 & -1 & -1 \\ 0 & 0 & 0 \\ 1 & 1 & 1 \end{bmatrix},\ y = \begin{bmatrix} -1 & 0 & 1 \\ -1 & 0 & 1 \\ -1 & 0 & 1 \end{bmatrix}, \quad (1)$$

as template operator. The X template operator is more sensitive to the vertical edge and the Y template operator is more sensitive to the horizontal edge.

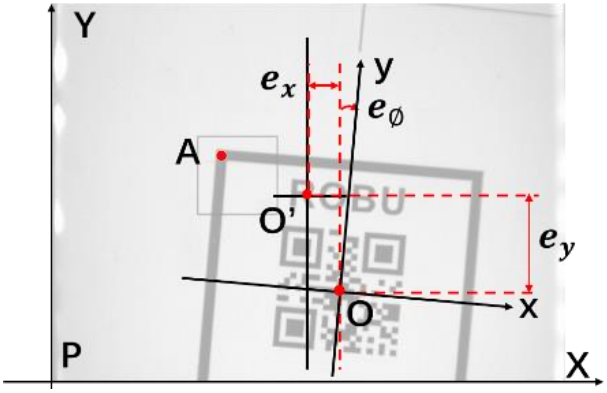

Figure 4 Position and orientation error

We use the X and Y templates to convolve the image and determine the gradient, respectively. f(x, y) represents the grey value of pixel (x, y). Gx and Gy represent the gradient of the point in X direction and Y direction,

$$G_x = \begin{bmatrix} -1 & 0 & 1 \\ -1 & 0 & 1 \\ -1 & 0 & 1 \end{bmatrix} * \begin{bmatrix} f(x-1,y-1) & f(x,y-1) & f(x+1,y-1) \\ f(x-1,y) & f(x,y) & f(x+1\ ,\ y) \\ f(x-1,y+1) & f(x,y+1) & f(x+1,y+1) \end{bmatrix}, \quad (2)$$

$$G_y = \begin{bmatrix} -1 & -1 & -1 \\ 0 & 0 & 0 \\ 1 & 1 & 1 \end{bmatrix} * \begin{bmatrix} f(x-1,y-1) & f(x,y-1) & f(x+1,y-1) \\ f(x-1,y) & f(x,y) & f(x+1\ ,\ y) \\ f(x-1,y+1) & f(x,y+1) & f(x+1,y+1) \end{bmatrix}, \quad (3)$$

$$|\mathbf{G}| = \sqrt{{G_x}^2 + {G_y}^2}\ . \quad (4)$$

The total gradient |**G**| of point (x, y) can be calculated with Eq.4. When |**G**| exceeds the setting threshold, the point (x, y) is regarded as an edge point. The result of edge detection is shown in Figure 5, green dots represent those edge points.

In order to calculate the pose deviation of the AGV more precisely, we classify the edges shown in Figure 5 into up, down, right and left direction, shown in Figure 6. Then according to the values of Gx and Gy shown in Figure 7, these edge points can correspond to the edges in the corresponding direction.

The edge points $((x_1, y_1),\ (x_2, y_2) \ldots (x_k, y_k))$ in up direction are selected to fit the up edge by using the least squares method. The straight line equation is shown as

$$y = kx + b, \quad (5)$$

Figure 5 Edge point

from which the dip angle can be calculated by

$$\alpha_{up} = \arctan(k). \tag{6}$$

Similarly, the same approach can be used for the edge points with down, right and left directions to obtain corresponding dip angles. which are represented by α_{down}, α_{right} andα_{left}. Thus, the orientation deviation $e_{\emptyset}$ can be calculated from

$$e_{\emptyset} = \frac{\alpha_{up}+\alpha_{down}+(\alpha_{right}-90)+(\alpha_{left}-90)}{4} \tag{7}$$

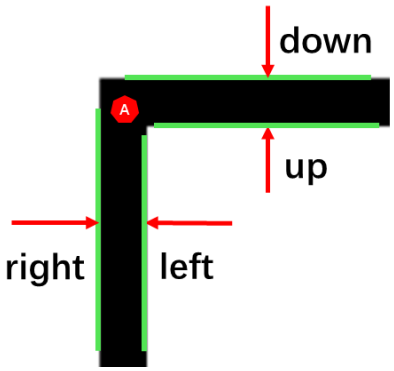

Figure 6 Four types of edge lines

To obtain the position deviation, the coordinate (x_A, y_A) of point A must first be calculated, as shown in Figure 4. Among all the edge points, point (x_1, y_1) depicts the edge point that is in the right gradient direction and has a maximal y coordinate. (x_2, y_2) represents the edge point in the left gradient direction that also has a maxima y coordinate. So x_A is equal to the mean of the values of x of these two points, that is

$$x_A = \frac{(x_1+x_2)}{2} \tag{8}$$

The same is true for y_A:

$$y_A = \frac{(y_3+y_4)}{2} \tag{9}$$

where y_3 and y_4 are the coordinates of the edge points in the up and down gradient directions, respectively, with minimal x. The experimental results are shown in Figure 8, in which the red dot is the calculated point A and the fitted straight-line is indicated in red.

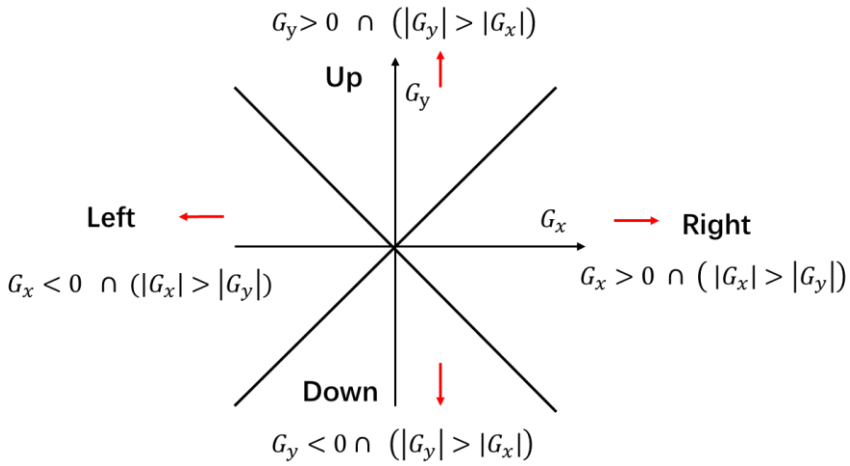

Figure 7 Directions of edge points

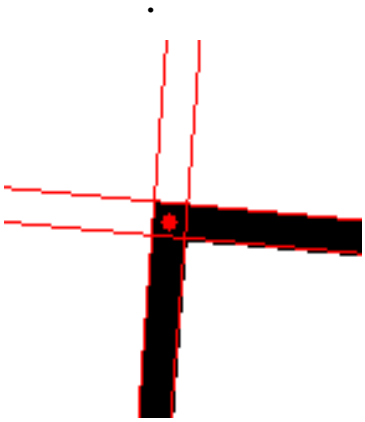

Figure 8 Straight line and corner point

Figure 4 shows the geometric relationship between points A and O. We can determine the position of O in the XPY coordinate system through the coordinates (x_c, y_c) of point A by transforming the coordinates. The position error is the deviation between the center of camera vision O' and the center of the landmark O, in both the X and Y directions. D is the length of the black border. The coordinates of A in the xoy coordinate system are (−D/2, D/2). This means that the coordinates of O in the XPY coordinate system can be calculated with the transforming coordinate equations,

$$x_O = x_A + \frac{D}{2} \times \cos(e_\emptyset) - \frac{D}{2} \times \sin(e_\emptyset), \tag{10}$$

$$y_O = y_A - \frac{D}{2} \times \cos(e_\emptyset) - \frac{D}{2} \times \sin(e_\emptyset). \tag{11}$$

The coordinates of point O', the center of camera view, are $(width/2, height/2)$. The position and orientation error can be calculated using the following equations:

$$e_x = x_O - x_{O'} \ , \tag{9}$$

$$e_y = y_O - y_{O'} \ . \tag{10}$$

The units of e_x and e_y obtained above are in pixels; the actual length of e_x and e_y can be calculated from the ratio of a given line's length to its corresponding segment's actual length.

RESULT OF IMAGE PROCESSING

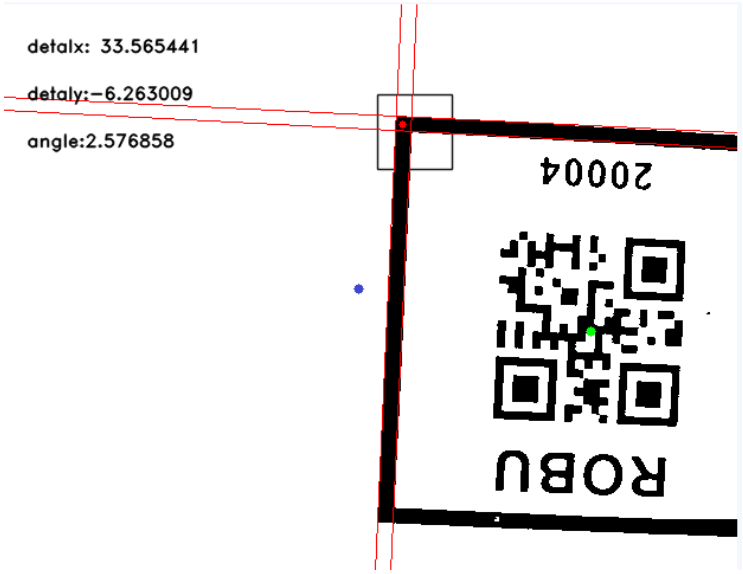

(a) The true value: detalx = 34.2 mm, detaly = 5.8 mm, angle = 2.66°

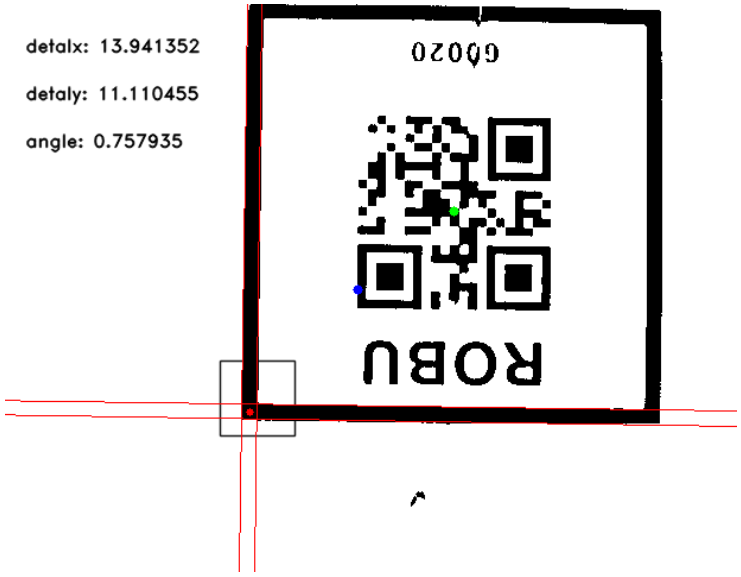

(b) The true value: detalx = 10.2 mm, detaly = 12.3 mm, angle = 0.86°

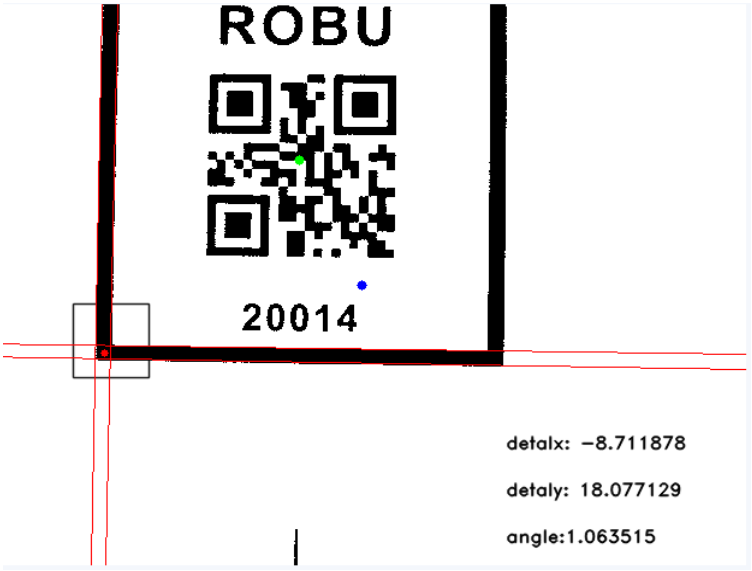

(c) The true value: detalx = 9.0 mm, detaly = 18.8 mm, angle = 0.93

Figure 9 The experimental results of pose deviation

The designs of the visual positioning method were programmed in C++. We have carried out many experiments to verify the accuracy of this method. In Figure 9, we show some of the results. Figure 9 contains 3 images, in which the position of landmark is different. The picture (a) in the Figure 9 displays the calculated pose deviation in the top right corner, where detalx is the position deviation e_x, detaly is the position deviation e_y and angle is the orientation deviation $e_{Ø}$. Compared with the true value of the pose deviation, it is obviously that the error between the calculated value and the true value is very small, so are the other two pictures. Abundant experiment has proved that our method has a measurement accuracy of positon error up to 3 mm and orientation error up to 1°. The detected ranges of errors are as follows: -70 mm $< e_x <$ 70 mm, -45 mm $< e_y <$ 70 mm, $-45°$ mm $< e_{Ø} <$ 45°.

CONCLUSION

In this paper, an efficient landmark-based visual positioning System of AGV is described. It can meet the requirements of accuracy and real time for AGV's positioning system. To maintain accuracy, we improve the edge extraction method based on Prewitt operator. We do not judge the edges by just roughly setting a certain threshold, but focus on the gradient direction of each pixel. The gradient directions of the edge points are redefined, with their directionalities divided into four categories. This clearly conforms each edge point to one of four edges of the landmark's black border and can help avoid misidentified points in line fitting. Points within the four edges are used to calculate the coordinates of imaged points to reduce error. Similarly, $e_{Ø}$ can be calculated as the average of the four edges' dip angles. Experimental results indicate that the accuracy of position deviation is 3 mm and that of orientation deviation is 1◦. Moreover, because this method is very concise and distinct, it can meet the requirement of real-time processing.

ACKNOWLEDGMENTS

This work was supported by the Cross-Disciplinary Research Innovation Fund under Grant JC20150002 from Graduate School at Shenzhen, Tsinghua University, the Singapore Ministry of Education Academic Research Fund Tier 2 (Grant No. MOE 2013-T2-2-033). The hardware is supported by Shenzhen ROBU Intelligent Technology Co., Ltd.v

REFERENCES

Angeloudis, P., Bell, M. G., 2010. An uncertainty-aware AGV assignment algorithm for automated container terminals. *Transportation Research Part E: Logistics and Transportation Review*, 46(3), 354-366.

Bosien, A., Venzke, M., and Turau, V. (2008, March). "A rewritable RFID environment for AGV navigation".*In Proceedings of the 5th International Workshop on Intelligent Transportation (WIT'08)*, Hamburg, Germany.

Borenstein, J., Everett, H. R., and Feng, L. (1996). "Where am I? Sensors and methods for mobile robot positioning". *University of Michigan*, 119(120), 27.

Bui, T. L., Doan, P. T., Park, S. S., and Kim, H. K. (2013). "AGV trajectory control based on laser sensor navigation". *International Journal of Science & Engineering*, 4(1).

Carelli, R., Soria, C., Nasisi, O., & Freire, E. (2002, November). Stable AGV corridor navigation with fused vision-based control signals. *In IECON 02 [Industrial Electronics Society, IEEE 2002 28th Annual Conference of the]* 3: 2433-2438 .

En-xiu, S. H. I., Huang, Y. M., Ying, Y. A. N., Liang, C. H. E. N., and Wen-hao, S. H. I. (2005). "Experiment study of AGV positioning based on ultrasonic sensors" [J]. *Journal of Transducer Technology*, 10, 007.

Fontanelli, D., Macii, D., Rizano, T. (2015) "A fast and low-cost vision-based line tracking measurement system for robotic vehicles". *Acta Agronomica Sinica* 40(10):1-13

Fazlollahtabar, H., Saidi-Mehrabad, M., 2015. Optimal path in an intelligent AGV-based manufacturing system. *Transportation Letters*, 7(4), 219-228.

Gelareh, S., Merzouki, R., McGinley, K., Murray, R. (2013) Scheduling of intelligent and autonomous vehicles under pairing/unpairing collaboration strategy in container terminals. *Transportation Research Part C: Emerging Technologies* 33:1-21.

Halle, S., Chaib-draa, B., 2005. A collaborative driving system based on multiagent modelling and simulations. *Transportation Research Part C: Emerging Technologies*, 13(4), 320-345.

Hartmann, S. (2013) Scheduling reefer mechanics at container terminals. *Transportation Research Part E: Logistics and Transportation Review* 51:17-27.

Hong, Y. (2010). "Research on AGV Based on Vision-based Navigation" [J]. *Foreign Electronic Measurement Technology*, 2, 017.

Jiangbo Du, Feng Xiong, Guoqing Qu, Junshi. (2016). "Research on agv positioning method based on VLC". *Industrial Control Computer*.

Juang, J. G., Wang, J. A. (2015) “Indoor map building by laser sensor and positioning algorithms”. *Applied Mechanics and Materials* 764-765:752-756

Luo, J., Wu, Y. (2015) “Modelling of dual-*cycle* strategy for container storage and vehicle scheduling problems at automated container terminals”. *Transportation Research Part E: Logistics and Transportation Review* 79:49-64.

Tabata, K., Nishida, Y., Iida, Y., Iwai, T. (2012) “New Navigation System for Automatic Guided Vehicles Using an Ultrasonic Sensor Array”. *Transactions of the Society of Instrument and Control Engineers* 48(1):11-19

Tang, J., Chen, Y., Jaakkola, A., Liu, J., Hyyppa, J., Hyyppa, H. (2014)” Navis-an ugv indoor positioning system using laser scan matching for large-area real-time applications”. *Sensors* 14(7):11805-11824

Ye, A., Zhu, H., Xu, Z., Sun, C., Yuan, K. (2012) “A vision-based guidance method for autonomous guided vehicles”. *International Conference on Mechatronics and Automation. IEEE* 2012:2025-2030